Catalysis Communications 132 (2019) 105804

Contents lists available at ScienceDirect

Catalysis Communications

journal homepage: www.elsevier.com/locate/catcom

Short communication

Facile synthesis of size-controlled Ag supported on WO_3 nanorods and their application as novel and active catalyst in oxidant-free dehydrogenation of benzyl alcohols

Bappi Paul[a], Sachin Sharma[a], Debraj D. Purkayastha[b], Siddhartha S. Dhar[b], Rajaram Bal[a,*]

[a] *Catalytic Conversion & Processes Division, CSIR-Indian Institute of Petroleum, Dehradun 248005, India*
[b] *Department of Chemistry, National Institute of Technology Silchar, Silchar 788010, Assam, India*

ARTICLE INFO

Keywords:
Ag-WO_3 nanorod
Polyethylene glycol
Size-tunable
Oxidant-free
Benzyl alcohols

ABSTRACT

A new and simple strategy for the size-tunable synthesis of silver supported tungsten oxide nanoparticles (NPs) was reported. Polyethylene glycol (PEG) of molecular weights 400 and 4000 was used as surfactant to tune the size of nanoparticles. These as-synthesized Ag/WO_3 nanomaterials were characterized by XRD, FT-IR, TGA, TEM, SEM, EDX, ICP-AES, XPS, and BET analysis. The material synthesized in the presence of PEG 4000 is ~10 nm metallic silver nanoparticles (Ag NPs) supported on tungsten oxide (WO_3) nanorods with diameters between 20 and 40 nm. These nanomaterials are very effective catalysts in oxidant-free dehydrogenation of benzyl alcohols.

1. Introduction

Synthesis and characterization of inorganic nanomaterials have received great interest and importance in various fields of science and technology [1–3]. It has also been observed that due to the synergistic effect, catalytic efficiency boost to great extent when nanomaterials doped with another metal [4]. Controlled and easy synthesis of Ag supported on WO_3 nanomaterials still poses great challenges despite significant research efforts. Development of a facile method for the in-situ synthesis of Ag supported on WO_3 nanomaterials with desired morphology, shape and size, is considered a challenging proposition. It is relevant to mention that polyethylene glycol (PEG) with ordered and uniform chained structure can act as a reducing agent as well as a surfactant to control morphology and size of the nanomaterials [5–7]. Previously PEG was used individually as a surfactant and reducing agent for the synthesis of WO_3 and Ag NPs. However, there has been no report on the use of PEG for the in-situ synthesis of Ag/WO_3 composites.

Numerous catalysts have been reported for the environmentally benign oxidation of alcohols. With the growing concern of economic and environmental acceptability, a process using atom economic catalyst system that does away with molecular oxygen or hydrogen peroxide for the conversion of alcohols to carbonyl compounds would be more attractive from an environmental standpoint. Such oxidant-free methodology is particularly useful from practical and commercial viewpoint due to (i) elimination of H_2O as by-products, which often cause work-up difficulty, (ii) its usefulness for O_2 and sensitive functional groups, (iii) production of H_2, that may be used as feedstock for energy generation (iv) its ability to prevent over oxidation to carboxylic acids [8–10]. A number of homogeneous as well as heterogeneous transition metal catalysis has been reported for oxidant-free dehydrogenation of alcohols [11–13]. A few homogeneous Rh [14], Ru [15] and Ir [16] based catalysts have been reported, but most of them suffer from the requirement for excess amount of base, high temperatures ($> 200\,^{\circ}C$), intense energy source, difficult catalyst synthesis and manipulation, difficulties in catalyst reuse, and high price. There are several heterogeneous catalyst based on Ru [17], Au [18], Ni [19], Cu [20] and Co [21] have also been documented in the literature and in most of the cases, the catalytic systems suffer from air sensitivity, low catalytic activity, harsh conditions, difficult catalyst synthesis, high catalyst loading, relatively poor activity and selectivity. Moreover, TOFs of these catalysts for production of aldehydes are not very high and thereby leaves scope for improvement. All these aforementioned limitations of literature reported on homogeneous and heterogeneous catalysts for dehydrogenative oxidation of alcohols provide enough scope for improvement in synthesis of a new catalytic system capable of exhibiting very strong performance. We report herein, a novel and facile method for the synthesis of Ag/WO_3 using PEG that plays a dual role of surfactant as well as reducing agent and studied their catalytic activity for dehydrogenation of benzyl alcohols.

---

* Corresponding author.
E-mail address: raja@iip.res.in (R. Bal).

https://doi.org/10.1016/j.catcom.2019.105804
Received 17 May 2019; Received in revised form 22 August 2019; Accepted 27 August 2019

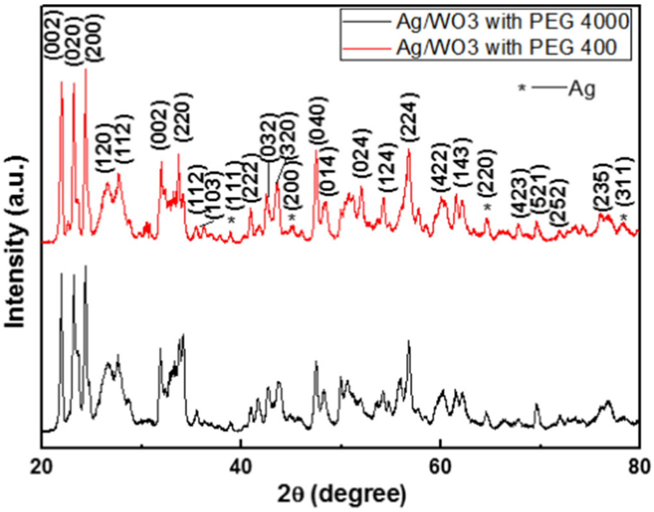

Fig. 1. Powder XRD patterns of Ag/WO_3 nanostructures.

2. Experimental

2.1. Synthesis of Ag/WO_3 nanostructured catalyst in presence of PEG 400 and PEG 4000

In a typical procedure, 1.25 g of H_2WO_4 (0.5 mmol) and 0.016 g of $AgNO_3$ (0.1 mmol) were dissolved separately in a distilled water and mixed together. Subsequently, 1 mmol of surfactant PEG 400 or PEG 4000 was added to the mixed solution. The pH was adjusted to ~9 by drop wise addition of NH_4OH solution. After 4 h of continuous stirring, the yellow suspension was collected, washed with water/ethanol and dried. The as-obtained solid powder was then calcined at 500 °C for 4 h in a muffle furnace.

2.2. General procedure for the dehydrogenation of benzyl alcohols using nanostructured Ag/WO_3

Is discussed in the supporting information of the manuscript.

3. Results and discussion

Ag supported on WO_3 nanocatalyst was synthesized in an aqueous medium using tungstic acid and silver nitrate as precursor sources for W and Ag, respectively. The main advantage of the synthesis procedure is the in-situ synthesis of Ag/WO_3 where no external reducing agent is used, and the PEG played a dual role of surfactant and reducing agent for Ag(I) (Scheme S1 in ESI). The same method has been proved to be effective for large scale synthesis of the catalyst (batch scale up to 20 g).

The powder XRD patterns were recorded for identification of phases exhibited by the synthesized materials. Fig. 1 shows the powder XRD patterns of the synthesized Ag/WO_3 catalyst. The diffraction peaks matched well with the orthorhombic phase of WO_3 (JCPDS File no. 89–4480, Fig. S1 in ESI). In addition, four diffraction peaks of face-centered cubic Ag at 2θ values of 38.92, 44.98, 64.57, and 78.25 corresponds to (111), (200), (220), and (311) planes were observed (JCPDS File no. 87–0720, Fig. S2 in ESI). The average crystallite sizes of the synthesized NPs were estimated by the Debye-Scherrer equation and were found to be 6.4 nm, and 8.72 nm modified with PEG 400 and PEG 4000 respectively.

The SEM images of the catalysts prepared by PEG 400 and PEG 4000 are shown in (Figs. S3(a)) and S4(a) in ESI, respectively. The images clearly indicate the formation of nearly uniform rod-like morphology of the WO_3 nanorod dotted with metallic Ag particles. The TEM image of the nanomaterial synthesized in the presence of PEG 400 (Fig. S3 (b and c)) shows Ag NPs of approximately sizes 20 nm randomly attached over WO_3 nanorods with diameter 100–350 nm. The fringes was found to be separated by 0.39 nm and 0.21 nm, possibly due to (002) the (200) plane of WO_3 and metallic Ag respectively. Single crystalline nature of the material was indicated by the electron diffraction (ED) pattern. The composite synthesized in the presence of PEG 4000 (Fig. S4 (b and c)) also showed the rod-like structure of WO_3 but with the much smaller diameter of 20–40 nm and Ag NPs of sizes nearly 10 nm deposited over WO_3 nanorods. The lattice fringes were found to be separated by 0.38 nm and 0.2 nm, possibly due to the (002) and (200) plane of WO_3 and metallic Ag, respectively. ED pattern indicated single-crystalline nature of the material. The corresponding particle size histogram of Ag (Figs. S3(f) and S4(f)), for catalysts prepared with PEG 400 and PEG 4000, respectively, exhibits narrow size distribution of the catalysts between 16 and 20 nm and 6–10, respectively. Thus surfactant PEG of higher molecular weight i.e. PEG 4000 has a superior effect in controlling the dimension and dispersity of Ag/WO_3 nanostructures. Further evidence of the formation of Ag NPs supported on WO_3 nanorod is provided in Fig. 2, which clearly shows that considerable numbers of Ag NPs are attached to the WO_3 nanorods. The EDAX patterns (Fig. S5 (a,b) in ESI) also indicated the existence of Ag, W, and O in the synthesized materials. The amount of Ag loaded in the catalysts was analyzed using ICP-AES technique.

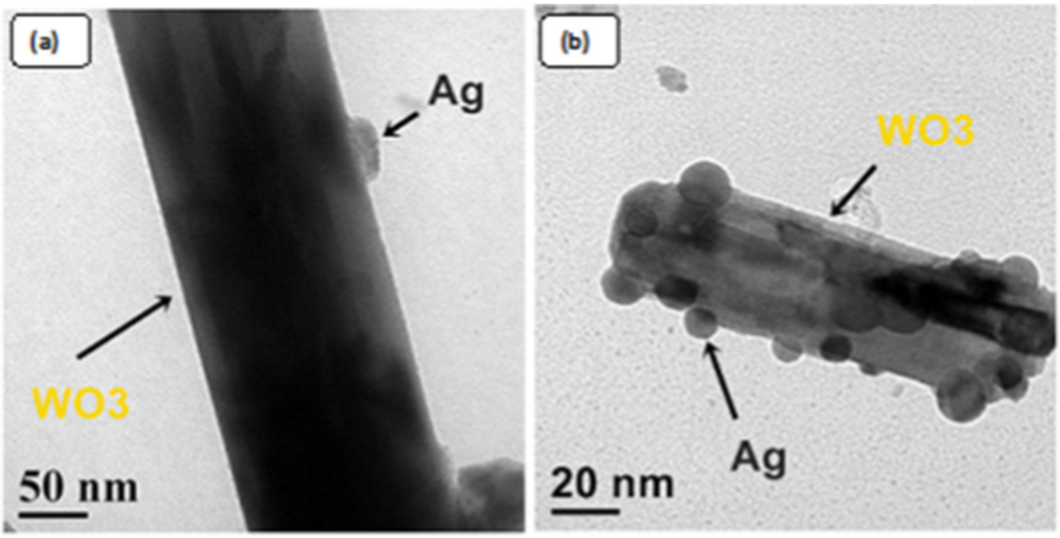

Fig. 2. TEM images confirming the attachment of Ag particles over WO_3 rod modified with (a) PEG 400, (b) PEG 4000.

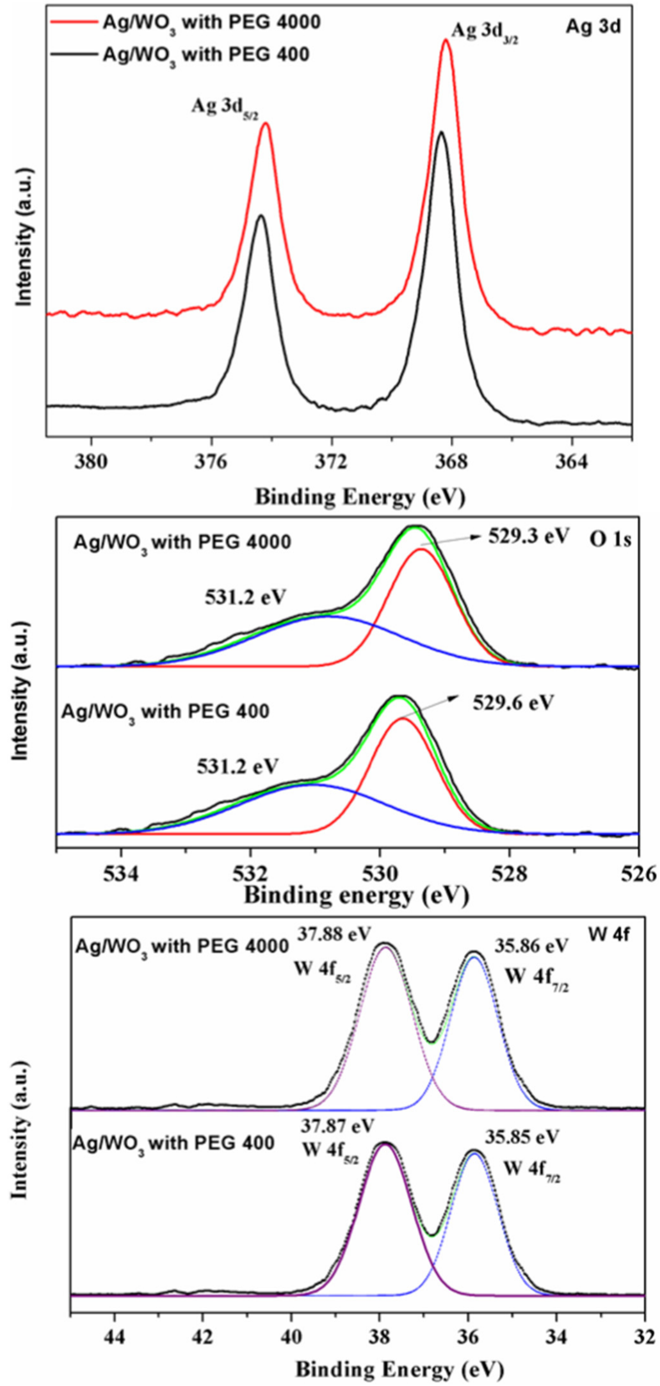

Fig. 3. XPS spectra ofAg particles over WO_3 rod modified with PEG 400 and PEG 4000.

Table 2
Catalyst amount, base, solvent optimization with 4-methyl benzyl alcohol.

Entry	Catalyst (wt%)	Base (Eq. amount of catalyst)	Solvent	Temp (°C)	Time (h)	Yield (%)
1	0.5	NaOH	Toluene	110	3	62
2	0.5	$Ba(OH)_2$	Toluene	110	3	26
3	0.5	Na_2CO_3	Toluene	110	3	15
4	0.5	Et_3N	Toluene	110	3	10
5	0.5	KOH	Toluene	110	3	96
6	0.1	KOH	Toluene	110	3	42
7	0.3	KOH	Toluene	110	3	84
8	0.5	KOH	DMSO	190	3	76
9	0.7	KOH	Toluene	110	3	93
10	1.0	KOH	Toluene	110	3	94
11	0.5	KOH	EtOH	75	3	0
12	0.5	KOH	CH_3CN	82	3	32
13	–	KOH	Toluene	110	3	20
14	0.5	Cs_2CO_3	Toluene	110	3	27
15	0.5	NaOH	DMSO	190	3	74
16	0.5	None	Toluene	110	3	0
15	0.5	K_2CO_3	Toluene	110	3	32

X-ray photoelectron spectroscopy (XPS) was performed to identify the valence state of Ag modified with PEG 400 and 4000 in Ag/WO_3 (Fig. 3). We can observe the metallic phase of silver as Ag $3d_{5/2}$ and Ag $3d_{3/2}$ with the binding energy around 368.1 eV and 374.2 eV with a slight shift to lower binding energies for the sample modified with PEG 4000 indicating a strong interaction between the silver nanoparticles and WO_3 nanorod.

We measured the BET surface area of the Ag/WO_3 synthesized with PEG 4000 and PEG 400 nanostructure catalyst, which gives the value 52.65 $m^2\,g^{-1}$ and 18.52 $m^2\,g^{-1}$ respectively. Where the surface area of the conventional Ag/WO_3 catalyst is only 5 $m^2\,g^{-1}$ [5]. The results are summarized in table (Table S1 in ESI).

The surface-coordinating of the organic molecules on the precursor synthesized in the presence of PEG were recorded by the FT-IR spectra. The precursor PEG 4000 showed stretching O—H band around 3448 cm^{-1} and a stretching vibrations band of a methylene group (C—H) at 2851 cm^{-1}(Fig. S6(a) in ESI). The sharp band at 1405 cm^{-1} may be due to H—C—H deformation of the PEG molecule. Band at 1105 cm^{-1} corresponds to C—O—C stretching vibrational mode. Similar FT-IR bands (Fig. S6(b) in ESI) were observed for the precursor synthesized in the presence of PEG 400. This confirms the presence of surfactant PEG on the surface of the precursor. However, after thermal treatment, the absence of these peaks reflects the complete removal of PEG molecules (Fig. S6(c) in ESI). This fact is further confirmed from the TGA results (Fig. S7 in ESI).

3.1. *Catalytic activity of nanostructured Ag/WO_3 for dehydrogenation of benzyl alcohols*

After successful synthesis and characterization of nanostructured Ag/WO_3, catalytic activity for dehydrogenation of benzyl alcohols was examined. The dehydrogenation of 4-methyl benzyl alcohol was carried out using (0.5 wt% of active catalyst) Ag/WO_3 synthesized with PEG 400 as well as PEG 4000, respectively. Results indicate that Ag/WO_3 synthesized with PEG 4000 exhibit superior catalytic activity in terms of yield, the selectivity of the product (Fig. S8). From this observation, it can be stated that the size and morphology of Ag/WO_3 nanostructure (Table 1) play an important role in the catalytic activity. WO_3 nanorods with diameter ~20–40 nm served effectively as a platform for higher dispersion of small-sized Ag NPs (~10 nm). Due to the higher efficiency of Ag/WO_3 with PEG 4000 catalyst, all the catalytic reaction was performed with the same catalyst.

Table 1
A comparative study of the catalysts synthesized by PEG 4000 and PEG 400 on dehydrogenation of 4-methylbenzyl alcohol.

Entry	Catalyst	Morphology	Size WO_3 (nm)	Size Ag (nm)	Surface area ($m^2\,g^{-1}$)	Time (h)	Yield (%)	Selectivity (%)	TOF (3 h) (h^{-1})
1	PEG 400	Rod shape	100–350	20	18.52	3	93	> 99	105
2	PEG 4000	Rod shape	20–40	10	52.65	3	96	> 99	108

Table 3
Catalytic dehydrogenation of benzyl alcohols in presence of PEG 4000 modified nanostructured Ag/WO_3.

Substrate	Product	Time (h)	Yield (%)	Selectivity (%)	TOF (3h)(h^{-1})
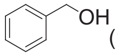 (1)	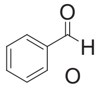 (1a)	6	98	>98	111
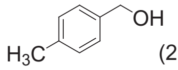 (2)	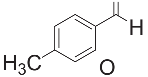 (2a)	3	96	>99	108
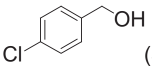 (3)	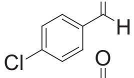 (3a)	6	94	>99	106
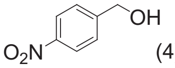 (4)	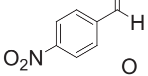 (4a)	4	93	>99	105
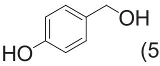 (5)	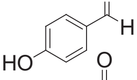 (5a)	6	92	>99	104
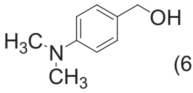 (6)	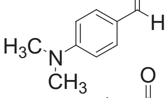 (6a)	4	99	>99	112
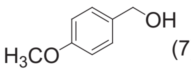 (7)	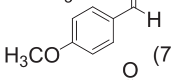 (7a)	4	96	>98	108
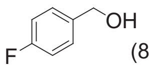 (8)	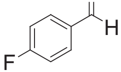 (8a)	6	92	>98	104
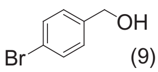 (9)	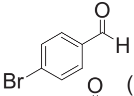 (9a)	7	90	>98	102
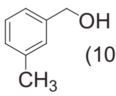 (10)	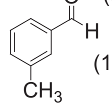 (10a)	4	96	>99	108

In order to optimize the reaction conditions, 4-methyl benzyl alcohol was chosen as a standard compound and various parameter such as solvent, temperature, base, and active catalyst amount were studied (Table 2). It may be mentioned that a very small amount of a base such as KOH equivalent to the amount of Ag present in the catalyst is required to initiate the reaction. The effect of the catalyst was investigated with varying amount of NPs from 0.1 to 1 wt%. Increasing the amount of catalyst up to 0.5 wt%, we observed a sharp increase in the yield and further increase in the catalyst amount did not observed any significant rise in yield. Best results were obtained when the catalyst amount of 0.5 wt% is refluxed at 110 °C in the presence of dry toluene as a solvent. C-balance and material balance were carried out for most of the experiment, and it was found that the error is ± 2%. The yield of the aldehyde in the absence of catalyst is very poor even after long reaction time.

Thus, taking into consideration the activity of Ag/WO_3 with PEG 4000 catalyst and standard optimized parameter, the reaction was further explored for various other substituted alcohols (Table 3). Various substituted benzyl alcohols bearing electron-donating groups and electron-withdrawing were examined. The *p*-substituted electron-donating groups showed pronounced activity with high yield compared to the electron-withdrawing groups. A gas burette fitted with H_2 detector was used to detected and measured the hydrogen gas evolved during the reaction. The volume of evolved hydrogen gas was measured using a gas burette, and the results are found to be consistent with the theoretical value. The individual role of Ag and WO_3 was explored, for which a series of catalytic reaction were conducted. Commercial Ag_2O and WO_3 exhibited very poor catalytic activity while bare Ag and WO_3 NP prepared with PEG assisted method did not show catalytic performance. Conventional catalysts prepared by impregnation method showed negligible activity. Negligible catalytic activity is shown by Ag supported commercial WO_3 NPs (Table S2 in ESI). The negligibly poor catalytic activity of commercially available catalysts, as well as catalysts prepared by impregnation method, may be attributed to irregular shapes and relatively larger sizes of particles that inhibit the access of reactants (Fig. S9 in ESI). The excellent catalytic activity of Ag/WO_3 with PEG 4000 synthesized by the present method may be due to high dispersion of Ag NPs supported on WO_3 nanorod and high specific surface area which leads to easy accessibility of the active catalytic sites and the reactants. Moreover due to the one dimensional structure, the catalyst activity is enriched in coordinatively unsaturated sites and the high exposed planes with lattice fringes played a crucial role in performing high catalytic activities. Table S3 in ESI provides the comparison between our work and some of the previously reported methods for the dehydrogenation of benzyl alcohol using a various catalyst and different reaction parameters.

Based on previous reports [9,22,23] on dehydrogenation of alcohols by Ag supported metal oxides, a proposed reaction is presented in Scheme S2 in ESI. KOH abstracts proton from the alcohol to yield an alkoxide group (RO^-) on the Lewis acid sites of tungstate oxide. The Lewis acid site of WO_3 is coordinated to the oxygen of the alkoxide group, and also a hydrogen-bonded with water molecules. It can be seen from the proposed scheme that Ag plays an important role in activation of C—H resulting in the formation of aldehydes and H_2 molecules.

3.2. Recyclability test

The solid catalyst was recovered from the reaction mixture by diluting with EtOAc, centrifuged and washed thoroughly with acetone and check the efficiency for multiple cycles. No significant decline in the activity even after 5 consecutive cycles was observed (Fig. S10 in ESI). Almost similar shape and size the catalyst was observed for the spent catalyst (Fig. S11 in ESI). Hot filtration test confirms no leaching of silver particles and true heterogeneity of the catalyst [24].

4. Conclusion

We have described here a novel, and facile synthesis of Ag NPs supported WO_3 nanorods. PEG 400 and PEG 4000 have been used to manipulate the dispersity of Ag particles over WO_3 nanorods as well as to control their sizes. Moreover, PEG has not only proven to be excellent surfactant but also the reducing agent for $AgNO_3$. The Ag/WO_3 nanomaterial exhibits very high catalytic activity for oxidant-free dehydrogenation of benzyl alcohols. PEG 4000 modified Ag/WO_3 catalyst are smaller in dimension and shows better activity in the dehydrogenation of benzyl alcohols with yield up to 98% with $> 99\%$ selectivity for aldehydes. The novelty of the present work lies in the facile synthetic procedure for Ag/WO_3 nanoparticles and their use as heterogeneous catalysts in the oxidant-free dehydrogenation of alcohols. Our present method is simple, reproducible, produce high yield (~98%), and large quantity catalyst (Ag/WO_3) can be prepared in a single batch.

Acknowledgement

B·P thanks SERB-DST, New Delhi, for financial support in the form of National Post-Doctoral fellowship of Project (PDF/2016/001948). Director IIP and NIT Silchar are acknowledged for his encouragementand support.

Appendix A. Supplementary data

Supplementary data to this article can be found online at https://doi.org/10.1016/j.catcom.2019.105804.

References

[1] Y.B. Miao, S.S. Wang, Size- and shape-dependent transformation of nanosizedtitanate into analogous anatasetitania nanostructures, J. Am. Chem. Soc. 128 (2006) 8217–8226.
[2] H.L. Sun, H.T. Shi, F. Zhao, L. Qi, S. Ghao, Shape-dependent magnetic properties of low-dimensional nanoscale prussian blue (PB) analogue $SmFe(CN)_6{\cdot}4H_2O$, ChemCommun. (2005) 4339–4341.
[3] S.M. Pourmertazari, M.R. Nasrabadi, M.K. Shalemzari, M.M. Zahedi, S.S. Hajimirsadeghi, I. Omrani, Synthesis, structure characterization and catalytic activity of nickel tungstate nanoparticles, Appl. Surf. Sci. 263 (2012) 745–752.
[4] D. Wang, Y. Li, Bimetallic nanocrystals: liquid-phase synthesis and catalytic applications, Adv. Mater. 23 (2011) 1044–1060.
[5] S. Ghosh, S.S. Acharyya, T. Sasaki, R. Bal, Fabrication of silver-tungsten wafer-like nanoarchitectures for selective epoxidation of alkenes, ACS Sustain. Chem. Eng. 3 (2015) 2823–2830.
[6] B. Paul, B. Bhuyan, D.D. Purkayastha, S.S. Dhar, Facile synthesis of α-Fe_2O_3 nanoparticles and their catalytic activity in oxidation of benzyl alcohols with periodic acid, Catal.Commun. 69 (2015) 48–54.
[7] C. Luo, Y. Zhang, X. Zeng, Y. Zeng, Y. Wang, The role of poly(ethylene glycol) in the formation of silver nanoparticles, J. Colloid Interface Sci. 288 (2005) 444–448.
[8] T. Mitsudome, Y. Mikami, K. Ebata, T. Mizugaki, K. Jitsukawa, K. Kaneda, Copper nanoparticles on hydrotalcite as a heterogeneous catalyst for oxidant-free dehydrogenation ofalcohols, Chem. Commun. 44 (2008) 4804–4806.
[9] M.H. Sarvari, T.A. Kachouei, F. Moeini, A novel and active catalyst Ag/ZnO for oxidant-free dehydrogenation of alcohols, Mater. Res. Bull. 72 (2015) 98–105.
[10] T. Mitsudome, Y. Mikami, H. Funai, T. Mizugaki, K. Jitsukawa, K. Kaneda, Oxidant-free alcohol dehydrogenation using a reusable hydrotalcite-supported silver nanoparticlecatalyst, Angew. Chem. Int. Ed. 47 (2008) 138–141.
[11] W.H. Kim, I.S. Park, J. Park, Acceptor-free alcohol dehydrogenation by recyclable ruthenium catalyst, Org. Lett. 8 (2006) 2543–2545.
[12] R. Kawahara, K.I. Fujita, R. Yamaguchi, Cooperative catalysis by iridium complexes with a bipyridonate ligand: versatile dehydrogenative oxidation of alcohols and reversible dehydrogenation–hydrogenation between 2-propanol and acetone, Angew. Chem. Int. Ed. 51 (2012) 12790–12794.
[13] K. Oded, S. Musa, D. Gelman, J. Blum, Dehydrogenation of alcohols under ambient atmosphere by a recyclable sol–gel encaged iridium pincer catalyst, Catal. Commun. 20 (2012) 68–70.
[14] S. Shinoda, T. Kojima, Y. Saito, $Rh_2(OAc)_4$-PPh_3 as a catalyst for the liquid-phase dehydrogenation of 2-propanol, J. Mol. Catal. 18 (1983) 99–104.
[15] G.R.A. Adair, J.M.J. Williams, Oxidant-free oxidation: ruthenium catalyzed dehydrogenation of alcohols, Tetrahedron Lett. 46 (2005) 8233–8235.
[16] K.I. Fujita, N. Tanino, R. Yamaguchi, Ligand-promoted dehydrogenation of alcohols catalyzed by Cp*Ir complexes. A new catalytic system for oxidant-free oxidation of alcohols, Org. Lett. 9 (2007) 109–111.
[17] J.H. Choi, N. Kim, Y.J. Shin, J.H. Park, J. Park, Heterogeneous shvo-type ruthenium catalyst: dehydrogenation of alcohols without hydrogen acceptors, Tetrahedron Lett. 45 (2004) 4607–4610.
[18] W. Fang, Q. Zhang, J. Chen, W. Deng, Y. Wang, Gold nanoparticles on hydrotalcites as efficient catalysts for oxidant-free dehydrogenation of alcohols, Chem. Commun. 46 (2010) 547–1549.
[19] M. Noda, S. Shinoda, Y. Saito, Liquid-phase dehydrogenation of 2-propanol by suspended nickel fine-particle catalyst, Bull. Chem. Soc. Jpn. 61 (1988) 961–965.
[20] T. Mitsudome, Y. Mikami, K. Ebata, T. Mizugaki, K. Jitsukawa, K. Kaneda, Copper nanoparticles on hydrotalcite as a heterogeneous catalyst for oxidant-free dehydrogenation of alcohols, Chem. Commun. 44 (2008) 4804–4806.
[21] Y. Uemichi, K. Shouji, M. Sugioka, T. Kanazuka, Highly effective dehydrogenation of cyclohexanol to cyclohexanone over carbon-supported cobalt catalyst, Bull. Chem. Soc. Jpn. 68 (1995) 385–387.
[22] K. Shimizu, K. Kon, K. Shimura, S.S.M.A. Hakim, Acceptor-free dehydrogenation of secondary alcohols by heterogeneous cooperative catalysis between Ni nanoparticles and acid–base sites of alumina supports, J. Catal. 300 (2013) 242–250.
[23] R. Rousseau, D.A. Dixon, B.D. Kay, Z. Dohnalek, Dehydration, dehydrogenation, and condensation of alcohols on supported oxide catalysts based on cyclic $(WO_3)_3$ and $(MoO_3)_3$ clusters, Chem. Soc. Rev. 43 (2014) 7664–7680.
[24] H.E.B. Lempers, R.A. Sheldon, The stability of chromium in CrAPO-5, CrAPO-11, and CrS-1 during liquid phase oxidations, J. Catal. 175 (1998) 62–69.